Flood Susceptibility Mapping and Engineering Exposure Assessment of Zhob District, Balochistan, Using Sentinel-1 SAR-Validated AHP and Frequency Ratio Modeling

A Flash-Flood Case Study Following the 2022 Pakistan Monsoon Floods

Jamil Rehman

Department of Civil Engineering, Balochistan University of Engineering and Technology, Khuzdar, Pakistan

Corresponding author: engrjamilrehman@gmail.com

Preprint Status

This manuscript is a non-peer-reviewed preprint submitted to EarthArXiv. It has not been submitted to, or accepted by, any peer-reviewed journal at the time of this posting. The author intends to submit this manuscript for peer review following posting of this preprint.

Abstract

Zhob District in northern Balochistan was substantially affected by the 2022 Pakistan monsoon floods, yet, unlike comparable districts mapped in the immediate aftermath of the same event (Larkana, Nowshera, Pishin, Quetta), it has lacked a dedicated, district-specific flood susceptibility assessment. This study addresses that gap using a hybrid Analytic Hierarchy Process (AHP) and Frequency Ratio (FR) approach, validated against an independently derived flood extent layer obtained from multi-temporal Sentinel-1 SAR change detection. Flood extent was identified by comparing an August 2022 flood-peak composite against a multi-year, same-month baseline (August 2019–2021), covering approximately 10.1 km² within the study area after speckle filtering, dual-polarization thresholding, connected-component cleanup, and a terrain-slope exclusion mask.

Rather than adopting factor-direction assumptions from lowland-floodplain literature, each conditioning factor's relationship to observed flooding was tested empirically via Frequency Ratio. This revealed that slope and Topographic Wetness Index behave contrary to the conventional flood-susceptibility pattern in this setting: steep terrain (FR = 3.80 in the steepest class) and low-TWI, fast-draining terrain (FR = 3.31 in the lowest class) show the strongest positive association with flooding, indicating a flash-flood regime originating in steep upper-catchment tributaries rather than gradual floodplain inundation. Factor directionality in the AHP model was corrected accordingly. The resulting susceptibility model achieved strong validation performance: 90.2% of SAR-confirmed flood pixels fell within the model's High and Very High classes, which together cover only approximately 40% of the study area — a discrimination ratio of 2.25 relative to random assignment, and consistent with validation levels reported for comparable regional AHP studies despite representing a fundamentally different flood mechanism.

The susceptibility surface was overlaid with OpenStreetMap road and settlement data to produce an engineering-oriented exposure ranking, identifying specific road segments — predominantly local and tertiary roads in the northwestern district rather than the primary N50 highway — and settlements at elevated flood risk. These results are intended to support drainage-structure review and maintenance prioritization by local infrastructure authorities. The principal contribution of this study is methodological as much as descriptive: it demonstrates that empirically testing, rather than assuming, conditioning-factor directionality is necessary in flash-flood-dominated mountainous catchments, where applying lowland-derived AHP conventions would misclassify the terrain most responsible for observed flooding.

Keywords: flood susceptibility; Analytic Hierarchy Process; Frequency Ratio; Sentinel-1 SAR; Zhob District; Balochistan; flash flood; road infrastructure exposure

1. Introduction

1.1 Background

Flooding is among the most recurrent and damaging natural hazards in Pakistan, driven by the interaction of intense monsoon rainfall, mountainous terrain, and limited drainage infrastructure. The 2022 floods were among the most catastrophic in the country's recorded history: monsoon rainfall exceeded seasonal averages by several multiples across Balochistan province, overwhelming river systems and reservoir capacity across dozens of districts placed under officially declared calamity status. Zhob District, situated along the Suleman mountain range in northern Balochistan, was among the affected areas, with the Zhob River and its tributary network swelling substantially during the event.

1.2 Literature Gap

GIS-based multi-criteria decision analysis — particularly the Analytic Hierarchy Process — is a well-established approach to flood susceptibility mapping in Pakistan's flood-prone regions. District-specific AHP-based studies have been produced for several Pakistani districts in the aftermath of the 2022 floods, including Larkana, Sindh (Khoso et al., 2025) and Nowshera, Khyber Pakhtunkhwa (Ashfaq et al., 2025). Within Balochistan specifically, comparable studies exist for Pishin District (Ashraf et al., 2025) and Quetta District (Ullah et al., 2024).

Notably, the Quetta study itself provides direct photographic documentation of 2022 flood damage in Zhob District, citing the closure of the national highway at Dhana Sar due to landsliding as illustrative evidence of province-wide impact, without Zhob itself being the subject of susceptibility analysis. Zhob's exposure during the 2022 event is therefore already acknowledged in the regional literature, yet no dedicated, district-specific susceptibility study exists for it, distinct from its inclusion in coarser national-scale flood-risk products. The Quetta study's own introduction further notes that no prior flood-mapping study existed for Balochistan or Quetta District as of 2024, underscoring how recent and sparse district-level flood susceptibility research remains in this province. This study addresses that specific gap for Zhob District.

1.3 Study Rationale and Civil Engineering Relevance

This study develops a flood susceptibility model for Zhob District using the 2022 flood event as its validation reference. Rather than relying on sparse historical event inventories — a limitation encountered even in the scoping of an alternative, landslide-based susceptibility approach considered for this same region during the initial stage of this research — the flood extent validation layer used here was derived directly from Synthetic Aperture Radar (SAR) change detection. This avoids dependence on incomplete news-media or citizen-science hazard catalogues, which are the principal constraint facing hazard mapping in under-studied regions such as this one.

The study is framed explicitly around civil-engineering decision support rather than hazard mapping in isolation. Susceptibility results are overlaid with road-network and settlement data to identify specific infrastructure exposed to elevated flood risk, producing a prioritized, ready-to-use output for maintenance planning and resource allocation rather than a purely descriptive hazard map.

1.4 Objectives

- Derive a validated flood-extent layer for Zhob District using multi-temporal Sentinel-1 SAR change detection for the 2022 monsoon flood event.
- Develop a flood susceptibility model for the district using a hybrid AHP–Frequency Ratio approach, with conditioning-factor directionality empirically validated against local flood evidence rather than assumed from general literature.
- Translate the resulting susceptibility surface into an engineering decision-support output by identifying specific road segments and settlements within high-risk zones.

2. Study Area

Zhob District, Balochistan, Pakistan (approximately 69.0–70.0°E, 30.9–31.8°N), was selected on the basis of its documented exposure during the 2022 Pakistan monsoon floods and the absence of any existing district-specific flood susceptibility study. The district lies within the Suleman mountain range in northern Balochistan and is drained by the Zhob River and its tributary network, which is characterized by a dense system of ephemeral, steep-gradient washes that carry flow only during intense rainfall — a terrain type materially different from the low-relief floodplain settings that dominate the comparator literature discussed in Section 1.2.

3. Methodology

3.1 Flood Extent Mapping (Validation Data)

Sentinel-1 SAR imagery (VV and VH polarization, Interferometric Wide swath mode) was used to detect flood extent during the 2022 monsoon event. To isolate flood-specific backscatter change from seasonal or vegetation-driven variation, a multi-year, same-month baseline approach was used: a composite of August imagery from three non-flood years (2019–2021) was compared against the August 2022 flood-peak window (22–31 August 2022), rather than relying on a single pre/post seasonal comparison, which would conflate inter-annual vegetation and soil-moisture variability with flood-driven change. Both composites were smoothed with a focal-median filter (50 m radius) to reduce speckle noise. Candidate flood pixels were identified where both VV and VH backscatter showed a drop exceeding 3 dB relative to the baseline, following a threshold commonly used in SAR-based open-water detection (Twele et al., 2016).

Two refinement steps were applied beyond this initial dual-polarization threshold. First, a connected-component filter (minimum cluster size of 8 pixels, 8-connectivity) removed residual speckle artifacts that survive median filtering as small, spatially isolated clusters — a stricter threshold than the 4-pixel minimum used in early iterations of this workflow, adopted after visual inspection showed that a 4-pixel minimum still retained scattered false positives on steep, radar-shadowed slopes. Second, a terrain-slope exclusion mask (SRTM 30 m DEM, 15° cutoff) removed candidate pixels on steep terrain, since radar layover and shadow on slopes exceeding this threshold can mimic the low-backscatter signature of open water — a well-documented source of false positives in SAR flood mapping in mountainous terrain (Martinis et al., 2015). This slope mask removed approximately 68% of the pre-mask candidate area, concentrated on hillslopes with no plausible hydrological connection to flood inundation, and is treated here as a physically justified exclusion rather than a discretionary noise-reduction step.

An initial cross-check using Sentinel-2 NDWI was attempted but found unreliable for this event, since sediment-laden floodwater does not consistently produce the expected NDWI signature — a documented limitation of NDWI-based water detection under high-turbidity conditions (Ji et al., 2009). The JRC Global Surface Water Monthly History product was also evaluated as a validation reference but found not to extend into the 2022 study period at the time of analysis; nonetheless, cross-referencing the final SAR-derived mask against JRC's longer-term maximum-extent layer indicated that roughly one quarter of flood pixels fell within historically documented water-prone zones, with the remainder concentrated along ephemeral drainage lines absent from that multi-decadal optical record — a pattern consistent with, rather than contradictory to, the flash-flood regime this study subsequently identifies through Frequency Ratio analysis (Section 3.4).

The resulting SAR-derived flood extent covers approximately 10.1 km² (29,601 pixels at 20 m resolution, representing 0.11% of the approximately 9,494 km² study-area bounding box). This should be understood as the SAR-detectable flood signature rather than the complete flood extent, since SAR change detection has known limitations in urban or built-up areas, where structural backscatter can mask underlying surface change (Mason et al., 2010).

3.2 Predictor (Conditioning Factor) Layers

Six flood-conditioning factors were derived, all processed in Google Earth Engine: elevation and slope (SRTM 30 m DEM), Topographic Wetness Index (TWI, derived from HydroSHEDS flow accumulation), distance to stream network (derived via a Euclidean distance transform applied to a flow-accumulation-thresholded stream network), NDVI (Sentinel-2, pre-flood dry-season composite, April–May 2022), and total monsoon rainfall (CHIRPS, July–September 2022 sum). All layers were resampled to a common 30 m grid prior to analysis.

A Pearson correlation matrix was computed across all six factors (sampled at 50,000 random points) to check for multicollinearity; no factor pair exceeded $|r| = 0.8$, and all six factors were retained.

3.3 AHP Weighting

An Analytic Hierarchy Process pairwise comparison matrix was constructed based on factor-importance rankings informed by regional flood susceptibility literature. A comparable AHP-based flood susceptibility study conducted in Larkana District, Sindh — notably examining the same 2022 flood event referenced in this study, alongside the 2010 flood — found rainfall and distance to river to be the two most influential factors, reported as approximately 35% and 30% weight respectively in the study's results discussion (the study's AHP computation table separately reports 28% and 22% for the same two factors, a minor internal inconsistency in the source worth noting here for transparency), followed by slope (approximately 20%) and elevation (approximately 15%) (Khoso et al., 2025). This ranking is broadly consistent with the weighting adopted here.

3.3.1 Rationale for the Larkana Analog

It is acknowledged that conditioning-factor importance varies meaningfully by region and flood-generation mechanism. A comparable study in Nowshera District found distance from river, elevation, height above nearest drainage, and slope most influential, with rainfall weighted considerably lower at approximately 8% (Ashfaq et al., 2025) — a materially different weighting structure from the Larkana study. Given this documented cross-study variability, the Larkana precedent was selected over the Nowshera precedent as the initial reference for two specific reasons rather than by default: first, Larkana and Zhob share the same triggering event (the 2022 monsoon flood), whereas Nowshera's underlying event history and river-regulation context (situated on the regulated Kabul River system) differ substantially from Zhob's unregulated, steep-catchment drainage; second, Larkana's AHP structure weights rainfall and stream proximity most heavily, which — while ultimately requiring empirical correction in this study, per Section 3.4 — provided a defensible, literature-grounded starting hierarchy rather than an assumption without precedent. Initial factor weights were therefore set following the Larkana precedent as the closest available regional, methodological, and flood-event analog: rainfall (0.416), distance to stream (0.226), TWI (0.161), slope (0.095), elevation (0.063), and NDVI (0.039). The Consistency Ratio (CR = 0.027) confirmed the pairwise judgments were internally consistent, well below the $CR < 0.10$ threshold recommended by Saaty (1980).

Rather than relying solely on literature-derived weighting, factor directionality was subsequently and independently validated against local flood evidence (Section 3.4) precisely because of this documented cross-regional inconsistency in the comparator literature. The magnitude of the weights is therefore literature-informed, while the direction of each factor's influence is empirically derived from this study's own SAR-based flood evidence — a distinction maintained explicitly throughout the remainder of this paper.

3.4 Frequency Ratio Cross-Check and Factor-Direction Validation

Before finalizing the susceptibility model, each factor's assumed direction of influence — whether high or low values correspond to higher flood risk — was tested empirically using Frequency Ratio (FR) analysis against the SAR-derived flood extent. FR was computed by binning each factor into five percentile classes and comparing the proportion of flood pixels within each bin to the proportion of total study area within that bin, where FR greater than 1 indicates over-representation of flooding and FR less than 1 indicates under-representation.

This analysis revealed that two factors behaved contrary to conventional lowland-flood assumptions. Slope showed the strongest positive association with flooding at its steepest class (FR = 3.80 at 20.6–83.2°, versus FR = 0.38 at the flattest class), and TWI showed the inverse of its typical relationship, with the lowest-TWI, fast-draining, non-convergent class showing FR = 3.31, versus FR below 1 for higher-TWI classes. This pattern is consistent with a flash-flood-dominated hydrological regime originating in steep upper-catchment tributaries, rather than slow floodplain inundation in low-relief, high-convergence terrain — a mechanism physically plausible given Zhob District's mountainous drainage network and consistent with the terrain-driven flash-flood behavior documented elsewhere in the Suleman range. Slope and TWI's normalization direction in the AHP model were therefore set to match this empirically observed relationship rather than the conventional lowland-flood assumption.

Rainfall also showed an unexpected inverse relationship (FR = 2.39 at the lowest rainfall class, declining to FR = 0.03 at the highest), discussed in detail in Section 5.2. The rainfall factor's normalization direction was set to match the empirical FR relationship for internal consistency with the rest of the model. Distance to stream and elevation both behaved consistently with conventional flood-susceptibility assumptions — closer to stream indicating higher risk, and lower elevation indicating higher risk — and required no directional adjustment.

3.5 Susceptibility Map Generation and Classification

Each factor layer was normalized to a 0–1 scale, inverted where the empirically validated relationship in Section 3.4 required it, and combined using the AHP-derived weights via weighted linear summation to produce a continuous Flood Susceptibility Index. The index was classified into five susceptibility zones, from Very Low to Very High, using percentile breaks at the 20th, 40th, 60th, and 80th percentiles, so that each class represents approximately 20% of the study area by construction.

3.6 Validation Approach

Model performance was validated by calculating the proportion of SAR-confirmed flood pixels falling within each susceptibility class, with results reported in Section 4.2. Because the equal-area percentile classification means each class covers approximately 20% of the study area by construction, the ratio of observed capture rate to this baseline provides a straightforward, interpretable discrimination metric that does not depend on an assumed threshold, complementing the capture-rate statistic itself.

3.7 Engineering Application: Road and Settlement Exposure

Road network and settlement location data were obtained from OpenStreetMap via the OSMnx Python package for the study area. Susceptibility class values were sampled along each road segment and at each settlement point to produce a ranked exposure table, identifying specific road segments and communities within the highest susceptibility zones for maintenance and planning prioritization.

4. Results

4.1 Flood Extent (Validation Layer)

Multi-year SAR change detection identified approximately 10.1 km² of flood-affected area within the Zhob study bounding box (29,601 pixels at 20 m resolution, 0.11% of the approximately 9,494 km² bounding box area), concentrated primarily around Girdao, Mir Ali Khel, and Shaighalu, following drainage lines and floodplain margins rather than appearing as diffuse noise across the landscape. This flood signature should be understood as the SAR-detectable extent rather than the complete inundation footprint, given known SAR limitations in built-up areas.

4.2 Susceptibility Model Performance

The AHP susceptibility model, with factor directionality empirically corrected per Section 3.4, classified the study area into five zones of approximately equal area (approximately 20% each, by construction of the percentile-based classification). Validation against the SAR-derived flood extent showed strong discrimination: 61.7% of flood pixels fell within the Very High class and a further 28.5% within the High class, for a combined 90.2% of flood pixels captured within the top two susceptibility classes, which together cover approximately 40% of the total study area. This represents approximately 2.25 times better discrimination than random chance would predict, since a random assignment would place only 40% of flood pixels in two of five equal-area classes.

This validation result is comparable to, and numerically similar to, the validation reported for the Quetta AHP flood study, which found approximately 90% of historical flood events falling within its model's High and Very High risk zones (Ullah et al., 2024). This provides external corroboration that this model's overall discrimination is consistent with comparable regional studies, despite the substantially different factor-direction logic required in Zhob's flash-flood setting relative to Quetta's lowland-dominated pattern.

4.3 Frequency Ratio Findings and the Flash-Flood Signature

Frequency Ratio analysis of individual factors revealed a hydrological signature distinct from the lowland-floodplain pattern typically reported in the regional literature; the Quetta study, for example, explicitly found flooding concentrated in areas of low slope angle and low elevation (Ullah et al., 2024). In this study's data, the steepest slope class showed the strongest positive flood association observed across all factors (FR = 3.80), while the lowest-TWI, fastest-draining class showed the second strongest (FR = 3.31) — both indicating flash-flood behavior originating in steep upper-catchment terrain rather than gradual floodplain inundation. Distance to stream behaved consistently with conventional expectations, with FR declining smoothly from 1.94 near-stream to 0.10 far from stream. Rainfall's inverse relationship (FR =

2.39 at the lowest rainfall class, declining to 0.03 at the highest) is discussed as a likely CHIRPS resolution and terrain-complexity limitation in Section 5.2.

4.4 Engineering Exposure: Road Segments and Settlements

Overlaying the susceptibility map with the OpenStreetMap road network (Figure 1) identified a concentration of highest-risk road segments in the northwestern portion of the study area, in the vicinity of Sambaza and Akozai, at approximately 3.3–3.9 mean susceptibility class, with 100% or near-100% of sampled points falling in High or Very High classes, predominantly along unclassified and tertiary roads rather than the N50 primary highway itself (Table 1). Segments near Brunj (mean class 3.25, approximately 89% high-risk) and Viala Sharak (mean class 3.0) represent the highest-risk points closer to Zhob town and along more locally trafficked routes. Notably, the N50 primary highway corridor itself was not dominant among the highest-ranked individual segments, suggesting its alignment may already avoid the most severe terrain-driven risk zones, while smaller local and residential access roads in the northwest of the district carry disproportionately higher exposure.

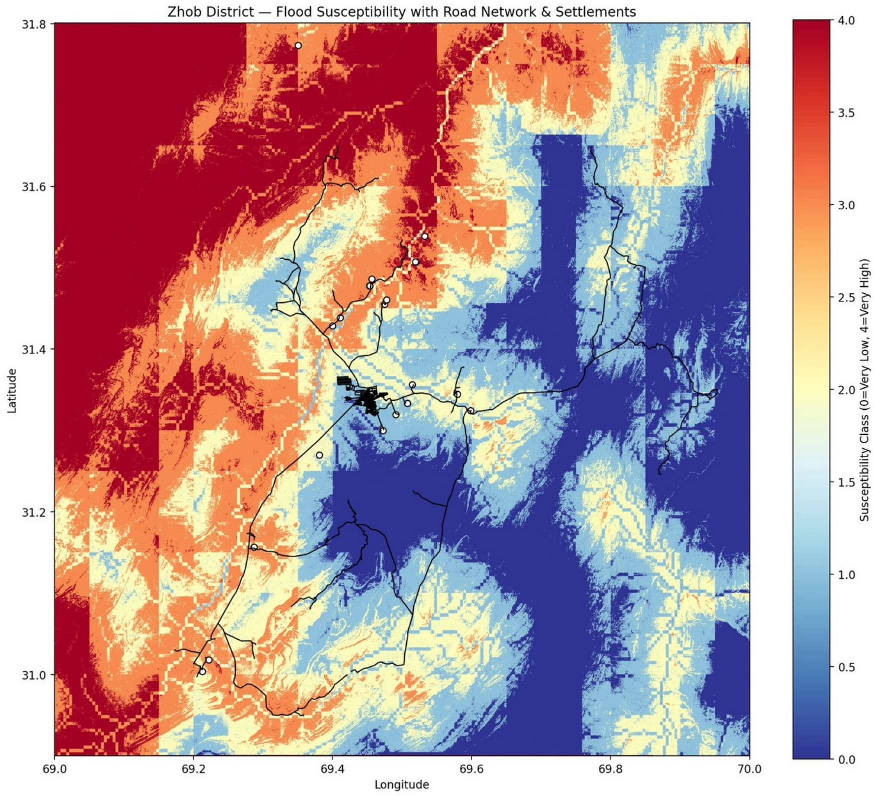

Figure 1. Zhob District flood susceptibility zones overlaid with OpenStreetMap road network (black lines) and settlement locations (white markers). Susceptibility class ranges from 0 (Very Low) to 4 (Very High).

Nearest Named Place	Road Type	Mean Susceptibility Class	% High-Risk Points
Sambaza (~15.9 km away)	Unclassified	3.91	100.0
Sambaza (~16.6 km away)	Unclassified	3.90	100.0
Sambaza (~16.1 km away)	Unclassified	3.73	100.0
Sambaza (~16.6 km away)	Unclassified	3.50	100.0
Akozai (~16.4 km away)	Primary	3.44	98.7
Sambaza (~16.5 km away)	Unclassified	3.33	100.0
Brunj (~2.1 km away)	Tertiary	3.25	88.8
Brunj (~2.2 km away)	Tertiary	3.25	88.8

Ali Khan Zai (~15.0 km away)	Unclassified	3.00	100.0
Viala Sharak (~0.2 km away)	Residential	3.00	100.0

Table 1. Top 10 highest-risk road segments by mean flood susceptibility class (0–4 scale) and percentage of sampled points falling in High or Very High classes. Full ranking (974 unique segments) available in the accompanying dataset (Zhob_road_segment_risk_ranking_v2.csv).

5. Discussion

5.1 A Flash-Flood, Not Floodplain, Hydrological Regime

The central empirical finding of this study is that Zhob District's 2022 flood behavior, as captured by SAR change detection, follows a flash-flood signature characteristic of steep, small mountainous catchments rather than the slow, low-relief floodplain inundation pattern that dominates the regional AHP literature, as seen in the Larkana and Quetta studies. This required departing from literature-derived factor-direction assumptions and instead deriving directionality empirically via Frequency Ratio (Section 3.4) — a methodological choice justified by, and consistent with, this being a fundamentally different flood mechanism than the lowland Indus-basin and urban-valley contexts examined in the comparator studies. This distinction matters beyond Zhob itself: it suggests that AHP-based susceptibility studies in other steep, upper-catchment districts of the Suleman and adjoining ranges should not assume lowland factor-direction conventions without an equivalent empirical check, since doing so risks systematically misclassifying the terrain most responsible for observed flooding as low-risk.

5.2 On the Rainfall Anomaly

The counterintuitive inverse relationship between CHIRPS seasonal rainfall and observed flood occurrence is plausibly explained by CHIRPS's documented, region-specific accuracy limitations. A dedicated evaluation of CHIRPS across Pakistan's Indus Basin found that the dataset's performance is spatially dependent, with substantially better accuracy in the Lower Indus Basin than in the topographically complex Upper Indus Basin, and that hydrological modelling using CHIRPS-derived rainfall over a mountainous test catchment resulted in systematic overestimation of streamflow relative to ground-gauge-driven simulations (Shahid et al., 2021). Since Zhob District lies within a similarly complex, mountainous drainage setting, it is plausible that CHIRPS's seasonal rainfall totals here are similarly biased or spatially displaced relative to the actual convective rainfall cells that triggered the 2022 flash flooding, rather than accurately representing localized peak-intensity rainfall at the sub-catchment scale relevant to flash-flood triggering. This is consistent with the broader finding that CHIRPS and comparable satellite rainfall products generally show reduced reliability in complex, sparsely gauged mountainous terrain.

A complementary, non-exclusive explanation is temporal rather than spatial: the fixed monsoon-season (July–September) rainfall total used here aggregates over a three-month window and cannot resolve the short-duration, high-intensity convective cells that trigger flash floods, since total seasonal accumulation and flood-triggering peak-intensity events are not necessarily co-located in either space or time. A sub-catchment that received a single extreme convective burst could register a modest seasonal total while still generating the peak discharge responsible for observed flooding, while a location with higher cumulative seasonal rainfall spread evenly across the monsoon may never reach flood-triggering intensity. Distinguishing between these two explanations — CHIRPS spatial bias versus temporal aggregation — is not possible with the data used in this study, and is identified explicitly as a priority for future work

(Section 6.2) rather than resolved here; both explanations are retained as plausible rather than the anomaly being treated as fully explained.

5.3 Robustness of Threshold Choices

The SAR flood-extent layer underlying this study's validation depends on several threshold choices made during preprocessing: the 3 dB dual-polarization change threshold, the 8-pixel connected-component minimum, and the 15° slope-exclusion cutoff. Each of these thresholds follows established convention in the SAR flood-mapping literature rather than being tuned specifically to maximize this study's validation statistic, which mitigates — though does not eliminate — the risk of threshold-driven overfitting between the flood-extent layer and the susceptibility model it validates. The slope mask in particular removed a substantial proportion of pre-mask candidate area (approximately 68%), and its effect on the downstream validation result (Section 4.2) has not been formally tested via sensitivity analysis across a range of threshold values. A systematic sensitivity analysis — re-running the validation statistic across a plausible range of change-detection and slope thresholds (for example, 2–4 dB and 10–20°) — would strengthen confidence that the reported 90.2% capture rate is not an artifact of a single threshold configuration, and is identified as a specific, tractable addition for a revised version of this study prior to journal submission.

5.4 Limitations

- Validation rests on a single flood event (2022) rather than a multi-year inventory, a limitation inherent to the SAR-derived validation approach adopted after NDWI and JRC Global Surface Water were both found unsuitable for this event.
- SAR-based flood detection has known limitations in urban and built-up areas.
- The 30 m / 20 m resolution of the underlying DEM and SAR data limits precision at the individual-structure scale.
- AHP weighting, even where empirically corrected via Frequency Ratio, retains some literature-informed subjectivity in the initial pairwise comparison structure (Section 3.3.1).
- The sensitivity of the validation result to specific preprocessing thresholds has not yet been formally tested (Section 5.3).

5.5 Engineering Implications

The finding that smaller, local roads in the northwestern district carry disproportionate flood exposure relative to the N50 primary highway has direct relevance for maintenance resource allocation and drainage design prioritization.

- Culvert and cross-drainage capacity review: the flash-flood signature identified in this study (Section 5.1) implies that drainage structures along the highest-risk unclassified and tertiary roads (Section 4.4) should be assessed for capacity against short-duration, high-intensity peak flows rather than steady-state seasonal discharge, since flash floods in steep catchments generate peak flows disproportionate to total seasonal rainfall volume. Culvert and cross-drainage sizing on these segments should follow standard hydraulic design practice using a design storm return period appropriate to the structure type. NHA Pakistan project-level hydrological design documentation specifies a 100-year design return period for bridges and a 50-year design return period for culverts (National Highway Authority, Pakistan, project design criteria); this standard is recommended as the basis for reviewing or upgrading drainage structures on the highest-risk segments identified in this study, noting that the applicable figure should be confirmed against the specific design manual governing the route in question.

- Prioritized inspection schedule: the ranked road-segment output (Section 4.4; full ranking in the accompanying dataset) provides a direct, ready-to-use prioritization list. Segments near Sambaza and Akozai (mean susceptibility class 3.3–3.9) warrant first-priority inspection and drainage capacity review ahead of the next monsoon season, followed by segments near Brunj and Viala Sharak.
- Differentiated design standards by risk zone: given that susceptibility classes correlate strongly with slope and drainage proximity (Section 4.3), new road construction or reconstruction within Very High and High susceptibility zones should incorporate slope stabilization and reinforced cross-drainage as standard design elements, rather than applying uniform district-wide design standards regardless of local terrain risk.
- Early warning and access resilience: since several of the highest-risk segments identified are local or unclassified roads rather than the N50 primary route, these roads likely serve as sole access for the settlements they connect, such as Sur Kach, Naweoba, and Badanzai. Maintenance planning should treat redundancy and rapid-repair capability on these segments as a life-safety priority, not only an infrastructure-preservation one, since their loss during a flood event may isolate communities rather than merely inconveniencing through-traffic.

6. Conclusion

This study developed a flood susceptibility model for Zhob District, Balochistan — a district demonstrably affected by the 2022 Pakistan monsoon floods, yet previously absent from the district-specific flood susceptibility literature that has otherwise covered comparable Pakistani districts in the same period. By deriving an independent, self-generated flood-extent validation layer from Sentinel-1 SAR change detection, this study avoided the historical-inventory data scarcity that constrains many hazard-mapping efforts in under-studied regions, instead grounding validation directly in observable 2022 flood evidence.

The central finding — that Zhob's flood behavior follows a flash-flood signature dominated by steep, fast-draining upper-catchment terrain rather than the low-relief floodplain pattern assumed in comparable regional AHP studies — was not an initial assumption but an empirical result, surfaced through systematic Frequency Ratio cross-checking of factor directionality against real flood evidence. This process led to substantively revising the initial literature-informed AHP weighting logic, and the resulting model achieved strong validation performance, with 90.2% of flood pixels falling within the top two susceptibility classes while those classes cover only approximately 40% of the study area — a result comparable to validation levels reported in established regional studies despite representing a fundamentally different flood mechanism.

Translating this susceptibility map into a ranked road-segment and settlement exposure table directly serves this study's civil-engineering framing: the finding that smaller, local, and tertiary roads in the northwestern district carry disproportionately higher flood exposure than the primary N50 highway is a concrete, actionable result for infrastructure maintenance prioritization, distinct from a purely descriptive hazard map. More broadly, this study demonstrates that empirically testing conditioning-factor directionality — rather than importing it from lowland-derived literature — is a necessary methodological step in flash-flood-dominated mountainous catchments, with implications extending beyond Zhob District to comparable terrain elsewhere in the Suleman range and similar steep, under-studied catchments.

6.1 Limitations, Restated

This study's conclusions should be read with several limitations in mind: validation rests on a single flood event rather than a multi-year inventory; SAR-based flood detection has known limitations in urban and built-up areas; the rainfall factor's counterintuitive behavior, while plausibly explained by documented CHIRPS accuracy limitations in complex Pakistani terrain, was not independently re-verified against ground-station rainfall data for Zhob specifically, and a temporal-aggregation explanation remains equally plausible (Section 5.2); the underlying 30 m / 20 m spatial resolution limits precision at the individual-structure or single-culvert scale; and the sensitivity of the reported validation performance to specific SAR preprocessing thresholds has not yet been formally quantified (Section 5.3).

6.2 Future Work

Future work could extend this study in four directions: incorporating ground-truthed rainfall station data, where available, to directly test the CHIRPS-limitation hypothesis proposed in Section 5.2, and to distinguish between the spatial-bias and temporal-aggregation explanations offered there; validating the model against additional flood events beyond 2022, should suitable SAR or optical imagery become available, to move beyond single-event validation; conducting a formal sensitivity analysis of the SAR preprocessing thresholds identified in Section 5.3 to quantify how strongly the 90.2% validation result depends on specific threshold choices; and extending the engineering exposure analysis to include drainage-infrastructure condition surveys, enabling direct comparison between modeled susceptibility and field-observed drainage-capacity deficits.

Declarations

Data Availability

The Sentinel-1 SAR, Sentinel-2, SRTM DEM, HydroSHEDS, and CHIRPS datasets used in this study are freely available through the Google Earth Engine data catalog. Road network and settlement data were obtained from OpenStreetMap via the OSMnx Python package. The derived flood-extent layer, predictor layer stack, susceptibility maps, and road/settlement risk ranking tables generated during this study are available from the corresponding author (engrjamilrehman@gmail.com) upon reasonable request.

Funding

This research received no specific grant from any funding agency in the public, commercial, or not-for-profit sectors. This study was conducted as independent, self-directed research using freely available satellite and open-source geospatial data.

Conflicts of Interest

The author declares no conflict of interest.

Author Contributions

Jamil Rehman: conceptualization, methodology, data curation, formal analysis, investigation, software, visualization, writing — original draft, writing — review and editing.

Acknowledgements

The author acknowledges the Department of Civil Engineering, Balochistan University of Engineering and Technology, Khuzdar, for institutional support, and the open-data providers whose freely available datasets made this independent study possible — the European Space Agency (Sentinel-1, Sentinel-2), NASA/USGS (SRTM), the Climate Hazards Center (CHIRPS), HydroSHEDS, and the OpenStreetMap contributor community.

References

Ashfaq, S., Tufail, M., Niaz, A., Muhammad, S., Alzahrani, H., & Tariq, A. (2025). Flood susceptibility assessment and mapping using GIS-based analytical hierarchy process and frequency ratio models. Global and Planetary Change, 251, 104831.

Ashraf, M., Shah, Q., Arshad, A., & Murtaza, G. (2025). Assessing hazardous flash flood susceptibility using multivariate zonation mapping techniques in Pishin District, Balochistan province of Pakistan. Natural Hazards, 121, 22935–22956. https://doi.org/10.1007/s11069-025-07723-0

Ji, L., Zhang, L., & Wylie, B. (2009). Analysis of dynamic thresholds for the normalized difference water index. Photogrammetric Engineering & Remote Sensing, 75(11), 1307–1317.

Khoso, W. A., Waseem, M., Tanoli, M. A., & Baig, F. (2025). Flood risk susceptibility analysis in Larkana district Pakistan using multi criteria decision analysis and geospatial techniques. Scientific Reports, 15, 13633. https://doi.org/10.1038/s41598-025-96107-2

Martinis, S., Kersten, J., & Twele, A. (2015). A fully automated TerraSAR-X based flood service. ISPRS Journal of Photogrammetry and Remote Sensing, 104, 203–212.

Mason, D. C., Speck, R., Devereux, B., Schumann, G. J.-P., Neal, J. C., & Bates, P. D. (2010). Flood detection in urban areas using TerraSAR-X. IEEE Transactions on Geoscience and Remote Sensing, 48(2), 882–894.

National Highway Authority, Pakistan. Design return period criteria for highway hydrological structures (bridges: 100-year; culverts: 50-year), as documented in NHA project design criteria. Retrieved from Pakistan Investment Portal project documentation, https://pakinvestment.com.pk/sector_read_more/26

Saaty, T. L. (1980). The Analytic Hierarchy Process. McGraw-Hill, New York.

Shahid, M., Rahman, K. U., Haider, S., Gabriel, H. F., Khan, A. J., Pham, Q. B., Mohammadi, B., Linh, N. T. T., & Anh, D. T. (2021). Assessing the potential and hydrological usefulness of the CHIRPS precipitation dataset over a complex topography in Pakistan. Hydrological Sciences Journal, 66, 1664–1684. https://doi.org/10.1080/02626667.2021.1957476

Twele, A., Cao, W., Plank, S., & Martinis, S. (2016). Sentinel-1-based flood mapping: a fully automated processing chain. International Journal of Remote Sensing, 37(13), 2990–3004.

Ullah, N., Tariq, A., Qasim, S., Panezai, S., Uddin, M. G., Abdullah-Al-Wadud, M., & Ullah, S. (2024). Geospatial analysis and AHP for flood risk mapping in Quetta, Pakistan: a tool for disaster management and mitigation. Applied Water Science, 14, 236. https://doi.org/10.1007/s13201-024-02293-1